Aerosol cloud interaction: a multiplatform-scenario-based methodology

Eduardo Landulfo[a], Fábio J.S. Lopes[b], Juan Luis Guerrero-Rascado[c,d], Lucas Alados-Arboledas[c,d]

[a]Instituto de Pesquisas Energéticas e Nucleares, Address, São Paulo, Brazil;
[b]nstituto de Astronomia, Geofísica e Ciências Atmosféricas de , Av Prof Lineu Prestes 2242, 05508000, São Paulo, Brazil;
[c]Universidad de Granada, Fuentenueva s/n, 18071, Granada, Spain;
[b]Instituto Interuniversitario De Investigación Del Sistema Tierra En Andalucía, Av. del Mediterrneo s/n, 18006, Granada (Spain), Granada, Spain;

ABSTRACT

Suspended atmospheric particles i.e. aerosol particles go through many chemical and physical processes and those interactions and transformations may cause particle change in size, structure and composition regulated by mechanisms, which are also present in clouds. These interactions play a great role in the radiation transfer in the atmosphere and are not completely understood as competing effects might occur which are known as indirect aerosol effects. Performing measurements and experiments in remote sensing to improve the knowledge of these processes are also a challenge. In face of that we propose a multi-platform approach based lidar, sun photometry and satellite observations which should be characterized under a scenario perspective in which given the cloud height, geometric and optical geometries in a diurnal/nocturnal basis will make possible to apply different analytical tools in each a set of product that specify the aerosol present in the vicinity of clouds, their optical and physical properties. These scenarios are meant to aid in tagging the expected products and help in creating a robust database to systematically study the aerosol-cloud interaction.In total we will present 6 scenarios: 3 under daylight conditions, 3 under at nighttime. Each scenario and their counterpart should be able to provide the cloud base/top height, aerosol backscattering profile and cloud optical/geometric thickness. In each instance we should count on a 5 wavelength Raman lidar system measurement, a collocated sun photometer and CALIPSO/MODIS observation from AQUA/TERRA platforms. To further improve the aerosol cloud interaction the Raman lidar system should have a water vapor channel or moreover a liquid water channel. In our study we will present a two-day case study to show the methodology feasibility and its potential application.

Keywords: Aerosols, clouds, indirect effect, lidar, satellites

1. INTRODUCTION

In order to forecast and understand better climate changes one has to quantify with good precision and accuracy the aerosol particles impact. These particles might be of natural or anthropic sources. The most import aspect is how do these particles affect cloud microphysics? Atmospheric aerosols go through many processes such as coagulation, phase transition, gas absorption and ultimately chemical reactions, which might occur in clouds, formed by coagulation of water vapor with pre-existing particles called *condensation nuclei* and *ice nuclei*.The cicles of primary and secundary formation, as well the removal processes are well known.[1] The **A**erosol- **C**loud-**I**nteraction is a major source of uncertainty as we put climate change in the main focus of discussion, and the mechanisms and interactions interplaying are several and complex.[1] As it is well known, the interactions to the date are: the increase in aerosol concentration that act as CCN can increase the droplet number in clouds, decreasing the droplet mean size for the same amount of liquid water, thus the cloud made of several and small droplets will reflect more incoming radiation as compared with a larger sized cloud droplet in smaller number.[2]

Further author information: (Send correspondence to E.L.)
E.L¿.: E-mail: elandulf@ipen.br, Telephone: 55 11 31339372

Lidar Technologies, Techniques, and Measurements for Atmospheric Remote Sensing XI, edited by Upendra N. Singh, Doina Nicoleta Nicolae, Proc. of SPIE Vol. 9645, 96450N
© 2015 SPIE · CCC code: 0277-786X/15/$18 · doi: 10.1117/12.2194130

Downloaded From: http://proceedings.spiedigitallibrary.org/ on 10/27/2015 Terms of Use: http://spiedigitallibrary.org/ss/TermsOfUse.aspx

As a consequence, an increase in aerosol load leads to a cloud reflectance augumentation, assuming that the water content stays constant. This effect is also known as *First Indirect Aerosol Effect* yields a negative forcing, i.e., cooling. On other hand a reduction in the collision-coalescence processes present in clouds with a great quantity of aerosols leads to a decrease in precipitation, *Albrecth Effect* or *Second Aerosol Indirect Effect*.[3] The precipitation suppression, or at least its extended permanency favours the cloud *lifting* to higher altitudes and enhances the water content with correspondent increase in optical depth and in reflectance.The last effect to mention is the *Semi-Direct Aerosol Effect* which is caused by particles higroscopic enough in such a way that cloud formation is inibited and its vertical development. This process affects the radiative balance considerably and is very sensitive to the vertical distribution of aerosols and clouds.[4–7] The aerosol effect on cloud optical depth and albedo still need to be further explored, and studies on the subject analysed insitu data obtained from airborne instruments used to observe relative humidity inside a cumulus cloud and an uprise in the scattering due higroscopicity ranging from 40 to 80 percent.[8] There are reports on the relation of aerosol optical depth and cloud droplet size obtained from satellite data, however there is no clear indication of how far apart aerosol layers and clouds were.[9] When using lidar data, studies concentrate in aerosols close to cloud base or cloud top when referring to satellite data. Evidences of an increase up to 20% in optical depth about 100 m from clouds, suggesting humidification and cloud formation processes to be present.[10] As speciation takes place like Saharan dust there is a trend in ice nucleation at temperatures less than 20^oC, verified by a polarization lidar.[11] Still under Saharan dust domain even layer-cloud distances ranging from 100 to 1000 m showed evidences of interaction increasing the challenge of treating clouds and aerosols layers as discrete entities.[12] CALIPSO data realized an increase in particle backscattering coefficient in a 15 km spatial domain around clouds and above the oceans, with a more pronounced increase in lower altitude clouds.[13] More recently a more dynamic scenario was shown[14] in an urban environment where cumulus clouds were contaminated by pollution and consequent increase in OD was observed. In this study we propose a methodology to study ACI with a muli-plataform remote sensing based in lidar, satellite and photometry instruments.

2. METHODOLOGY

The methodology showed here is based in diferent observational scenarios which employ distinct plataforms which would suit better to the conditions clouds and aerosols interact. Each one of these scenarios are depicted in a diagram shown in figure 1.

2.1 Scenario Description

The scenarios follow the availabilty of given plataform data: SATELLITE (CALIOP and/or MODIS), PHOTOMETRY (CIMEL sunphotometer) and lidar with the presence of clouds and the aerosol optical properties in their surroundings. The cloud properties to be observedare base and top height, cloud optical depth OD_{cloud} and cloud lidar ratio, S_{cloud}, and when available depolarization properties δ. The aerosol products are AOD_{aer}, extinction and backscatter coefficients, α_{aer} and β_{aer}, lidar ratio, S_{aer}, and N_{aer}*. The scenarios are organized as follows:

- I - Lidar diurnal measurements to retrieve top/base cloud heights of optically *thin* clouds, allowing the retrieval of AOD_{cloud} and S_{cloud}. Aerosol optical properties are retrieved at N_λ wavelengths. According to satellital overpasses CALIOP/TERRA/AQUA implement the cloud field in the retrieval area aided by sunphometric measurements after cloud screening data become available.
- II - Lidar diurnal measurements to retrieve top/base cloud height of optically *thick* clouds, allowing the retrieval of AOD_{cloud} and S_{cloud}. Aerosol optical properties are retrieved at N_λ wavelengths. Satellital overpasses CALIOP/TERRA/AQUA will implement the cloud field in the retrieval area aided by sunphometric measurements after cloud screening data become available.

*For multiwavelength lidar systems the $3\beta+2\alpha+\delta$ approach can be employed when a more complete set of microphysical parameters could be extracted.[15]

Downloaded From: http://proceedings.spiedigitallibrary.org/ on 10/27/2015 Terms of Use: http://spiedigitallibrary.org/ss/TermsOfUse.aspx

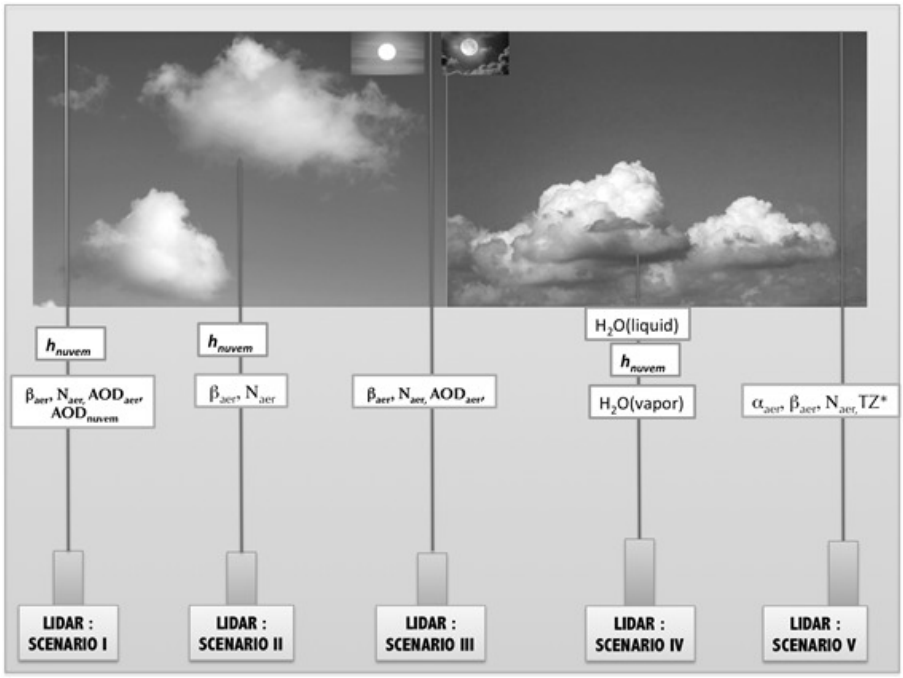

Figure 1. - Scenarios for selection and identification for an ACI analysis and corresponding products which could be extracted by each plataform used.

- III - Lidar diurnal measurements in a *cloud-free atmosphere*,i.e., no clouds in the laser beam path. AOD_{aer} and S_{aer} are retrievable and validated by CALIOP/TERRA/AQUA. Radiometric data helps in the aerosol closure. In a time-series sequence balance of population and de-population of aerosols induced from cloud scavenging.
- IV - Lidar nocturnal measurements to retrieve top/base cloud heights of *t*hin clouds, allowing the retrieval of AOD_{cloud} and S_{cloud}. Aerosol optical properties could be retrieved at N_λ wavelengths. Raman lidar measuremnts increase amount of information about particle microphysical properties plus water vapor profile and liquid water content.[16]
- V - Lidar nocturnal in cloud free conditions,AOD_{aer} and S_{aer} are retrievable and validated by CALIOP /TERRA/AQUA. In a time-series sequence balance of population and de-population of aerosol induced from cloud scavenging and *Twilight Zone* for inter-cloud aerosols observations.[5]

Some additional scenarios might be inspected if more equipment are brought to the detection array. The idea is to have a spatio-temporal analysys of the quantities retrieved in each situation to better comprehend the dynamics of ACI's.

3. INSTRUMENTS

The lidar system called MSP-Lidar, is located at Centro de Lasers e Aplicações (CLA) from the Instituto de Pesquisas Energéticas e Nucleares (IPEN $-23°$ 33' S, 46°44' W, 843 m above sea level), in the western region of So Paulo. The MSP-Lidar is a multiwavelength Raman lidar operating at CLA since 2001.[17,18] It is configured in a monostatic biaxial alignment pointing vertically to the zenith.

The transmission system consists of a pulsed Nd:YAG with fundamental emission at 1064 nm. Additional emissions at 532 and 355 nm are obtained from second and third harmonic generators. The backscattered signal

Downloaded From: http://proceedings.spiedigitallibrary.org/ on 10/27/2015 Terms of Use: http://spiedigitallibrary.org/ss/TermsOfUse.aspx

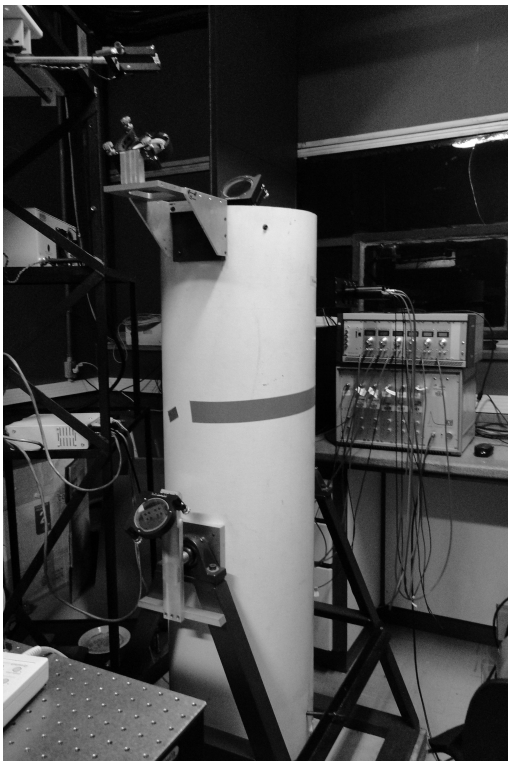

Figure 2. Lidar system used in this experiment.

is collected by a 30cm-diameter Newtonian telescope and split into six spectral channels using dichroic mirrors and interference filters. The detection and spectral selection is performed at these six channels corresponding to elastic wavelengths at 532 and 355 nm, and traditional channels for the Raman signals at 607 nm and 387 nm (N2 Raman-shifted signal from 532 nm and 355 nm) and 408 nm and 660 nm (water vapor Raman-shifted signal from 355 nm and 532 nm) and 387 nm (N2 Raman-shifted signal from 355 nm). The instrument is operating with a vertical spatial resolution of 7.5 m. Since 2008 the MSP-Lidar II system is part of LALINET (http://lalinet.org), that is a coordinated lidar network focused on the vertically-resolved monitoring of the particle optical properties distribution over Latin America.[19]

Table 1. LIDAR system setup.

Laser	
Laser type	Nd:YAG Laser (ICE 450/CFR)
Wavelengths	355, 532, 1064 nm
Pulse energy	100 mJ (355 nm), 200 mJ (532 nm) and 400 mJ (1064 nm)
Repetition rate	20 Hz
Pulse duration	(7 $\pm$ 2) ns
Receiver	
Optical design	150 mm diameter Cassegranian telescope
Focal length	1000 mm
Field of view	$\leq$ 1 mrad
Transient recorder	Licel (TR20-80) 10 - 250 MHz bandwidth

Downloaded From: http://proceedings.spiedigitallibrary.org/ on 10/27/2015 Terms of Use: http://spiedigitallibrary.org/ss/TermsOfUse.aspx

The CALIPSO satellite was launched in April 2006 and flies in a 705 km sun-synchronous polar orbit with an equator-crossing time of about 13:30 local solar time, covering the whole globe in a repeat cycle of 16 days.[20] The primary instrument aboard CALIPSO is the Cloud-Aerosol Lidar with Orthogonal Polarization (CALIOP), a two-wavelength laser (532 nm and 1064 nm) operating at a pulse repetition rate of 20.16 Hz.[21] The CALIOP data products are assembled from the backscattered signals measured by the receiver system and are divided in two categories: level 1 products and level 2 products. Level 1 products are composed of calibrated and geolocated profiles of the attenuated backscatter signal and are separated into the total attenuated backscatter profile at 1064 nm, the total attenuated backscatter profile at 532 nm (i.e., the sum of parallel and perpendicular signals) and the perpendicular attenuated backscatter signal at 532 nm.[20,22] The level 2 products are derived from the level 1 products and three different level 2 products are distributed according to the layer products, profile products and the vertical feature mask (VMF). The set of CALIPSO algorithms uses an aerosol classification scheme to assign each aerosol layer to one of the six aerosol types, namely dust, biomass burning, clean continental, polluted continental, marine, and polluted dust.[23] Several validation studies were conducted to show the accuracy of the CALIPSO aerosol classification scheme,[24–27] including in the South America region.[28]

The Moderate Resolution Imaging Spectrometer (MODIS) sensor is on board the polar orbiting satellites AQUA launched in 2002. The sensor was the first designed to obtain global observations of aerosols with moderate resolution (between 250 m and 1000 m depending on the wavelength used). MODIS has 36 spectral bands between 0.4 and 14.5 $\mu\,m$, allowing the generation of several products related to aerosol, such as aerosol optical depth over the ocean and land with a resolution of 10x10 km (at nadir), and the size and type distribution over oceans and type of aerosol over the continent.[29,30] In this study 550 nm AOD product from aerosol Level 2 were used.

The AErosol RObotic NETwork (AERONET)[31] is an international system of ground-based sun photometers that provides automatic sun and sky scanning measurements. Using direct sun measurements, AERONET provides both AOD and the Ångström Exponent (Å), which gives the wavelength dependence of the AOD. By using multiangular and multispectral measurements of atmospheric radiance and applying a flexible inversion algorithm,[32] the AERONET data can also provide several additional aerosol optical and microphysical parameters, such as size distributions, single-scattering albedo and refractive index. The operating principle of this system is to acquire aureole and sky radiance observations using a large number of solar scattering angles through a constant aerosol profile, and thus retrieve the aerosol size distribution, the phase function and the AOD.

4. RESULTS

To put the presented methodology in practice we have selected a day where a multiwavelength lidar was used in an urban atmophere in São Paulo, Brazil. The so-called Metropolitan Area of São Paulo, one of the largest megacities in the world, faces several problems related to the air quality due the high concentrations of aerosols produced either by local sources or by long-range transporting. Concerned with the elevated concentrations of aerosol and their impact in the air quality and the climate changes inside MASP, a measurement campaign were conducted during the South hemisphere winter of 2012, when the low temperatures and the low level of precipitation contribute to the poor dispersion of aerosols. From this campaign we have selected April 2^{nd}, 2015 as shown in figure 3 where 8 periods are indicated and each of them were classified following the scenario selection presented before. In figure 4, the first two periods, ① and ②, occurred during daytime amd are showed without and with clouds, respectively, thus they correspond to scenarios III and II, given the fact the cloud is not optically thin, the sunphotomoter was operational and presented a moderately high AOD about 0,15 and 0,20. The cloud top/base height were 1380 m and 800 m. And a careful inspection of the lidar backscatter profiles reveals a decrease below the cloud only in the UV profile which could be related to the low beam energy and the scavenging of smaller particles into the cloud base. The two following scenarios, given by figure 5, depict the same events as before, and periods ③ and ④, are similar, however the cloud is relatively less thick, about 170 m, and the cloud occur in the top of the mixing layer where the abundance of aerosols is larger. Periods ⑤, ⑥ and ⑦, ⑧ were obtained during nighttime, and correspond pairwise to scenarios IV and V, respectively, in figure6. Sunphotometer products are not available for obvious reasons and satellite products will not be presented in this example. The products for nighttime measurements include Raman scattering results: $\beta^{aer}_{355,532}(z)$,$\alpha^{aer}_{355,532}(z)$,$w\frac{H_2O}{N_2}(z)$,$S^{aer}_{355,532}(z)$. It is important to mention that while in daytime the lidar data are

Downloaded From: http://proceedings.spiedigitallibrary.org/ on 10/27/2015 Terms of Use: http://spiedigitallibrary.org/ss/TermsOfUse.aspx

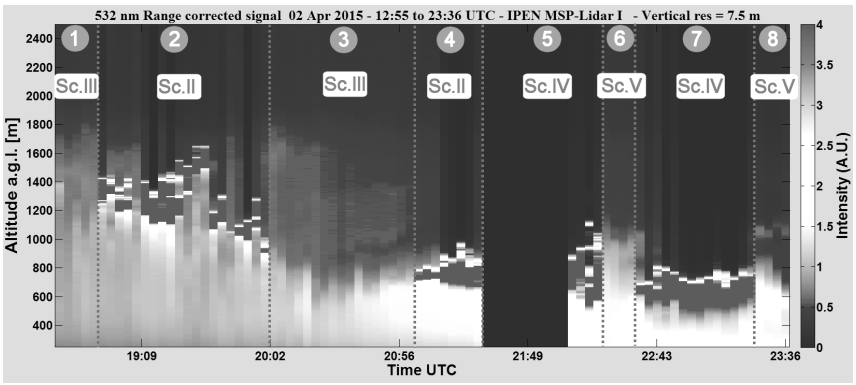

Figure 3. Period (numerals)- Scenario(roman) selection and identification for ACI analysis.

analysed using the *K*lett-Fernald Method[33,34] thus yielding an average lidar ratio, $\overline{S}^{aer}_{\lambda}$, in nighttime the lidar ratio is given as a profile or layer in the atmosphere, $S^{aer}_{\lambda}(z)$. Overall this approach helps in observing the dynamics involved in ACI, however, in pratical terms the filtering process will be extensive in identifying the different scenarios, and in terms of lidar signal the signal-to-noise ratio is an important pre-processing quantity as it will directly affect the lidar products obtained and the smoothed profiles. Also when obtaining the water vapor mixing ratio profiles, a cloud free calibration process should be performed.

Following their classification the lidar data allowed us to obtain the aerosol/cloud quantinties described in the scenarios descriptions and give in the table below.

Table 2. Scenario × Period classification plus the multi-plataform products.

Period	Scenario	Lidar Products[p]	Photometer Products
①	III	$\beta^{aer}_{355,532}(z)$,$\alpha^{aer}_{355,532}(z)$ & $\overline{S}^{aer}_{355,532}$	$AOD_{355,532}$
②	II	$\beta^{aer}_{355,532}(z)$ & $\alpha^{aer}_{355,532(z)}$,$Z^{cloud}_{top,base}$	$AOD_{355,532}$ from Period ①
③	III	$\beta^{aer}_{355,532}(z)$,$\alpha^{aer}_{355,532}(z)$ & $\overline{S}^{aer}_{355,532}$	$AOD_{355,532}$
④	II	$\beta^{aer}_{355,532}(z)$,$\alpha^{aer}_{355,532}(z)$,$Z^{cloud}_{top,base}$	$AOD_{355,532}$ from Period ③
⑤	IV	$Z^{cloud}_{top,base}$	N.A.
⑥	V	$\beta^{aer}_{355,532}(z)$,$\alpha^{aer}_{355,532}(z)^{r}$,$\frac{H_2O}{N_2}(z)$,$S^{aer}_{355,532}(z)$	N.A.
⑦	IV	$Z^{cloud}_{top,base}$	N.A.
⑧	V	$\beta^{aer}_{355,532}(z)$,$\alpha^{aer}_{355,532}(z)^{s}$,$\frac{H_2O}{N_2}(z)$,$S^{aer}_{355,532}(z)$	N.A.

[p] Å(532/355) additional
[r] Raman
[s] Raman

Downloaded From: http://proceedings.spiedigitallibrary.org/ on 10/27/2015 Terms of Use: http://spiedigitallibrary.org/ss/TermsOfUse.aspx

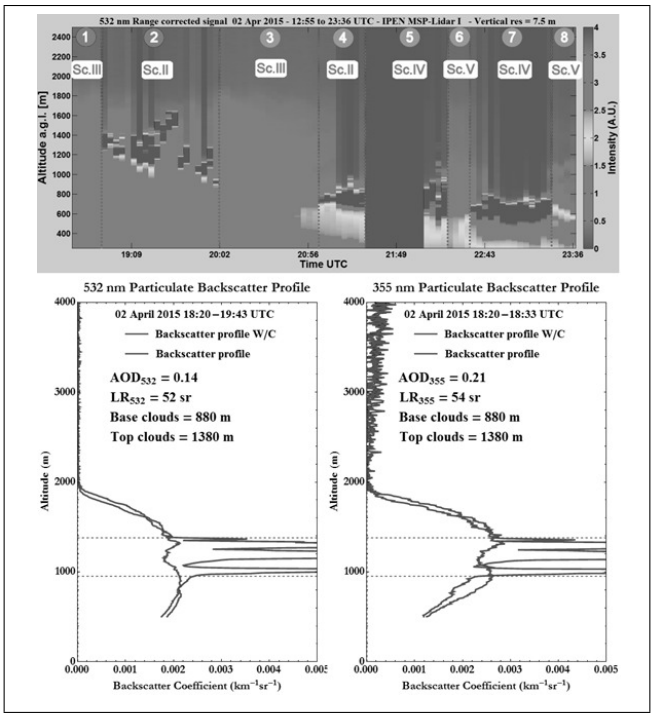

Figure 4. Periods ①,② - Scenarios III,II identification applied to a "curtain plot" (RCS plot) to apply the data extraction in order to observe ACI's. Below $\beta^{aer}_{355,532}$ with/out clouds.

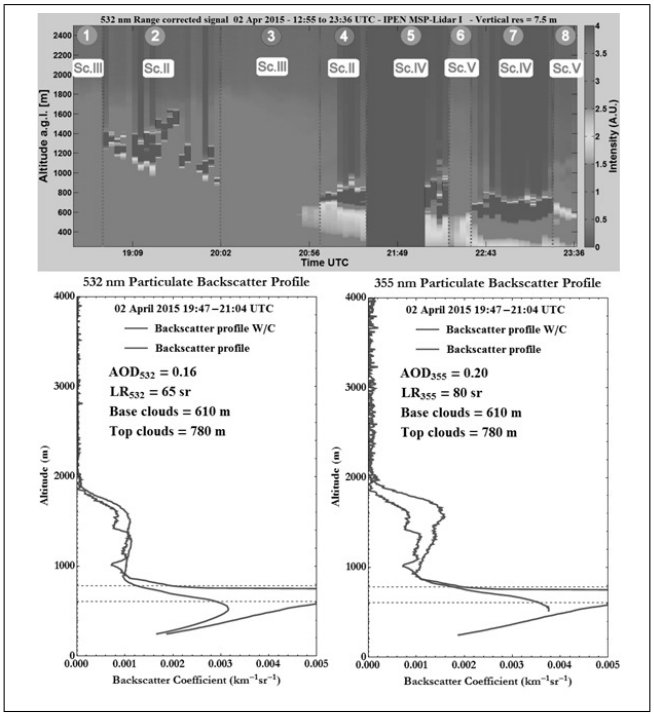

Figure 5. Periods ③,④ - Scenarios III,II identification applied to a "curtain plot" (RCS plot) to apply the data extraction in order to observe ACI's. Below $\beta^{aer}_{355,532}$ with/out clouds.

Downloaded From: http://proceedings.spiedigitallibrary.org/ on 10/27/2015 Terms of Use: http://spiedigitallibrary.org/ss/TermsOfUse.aspx

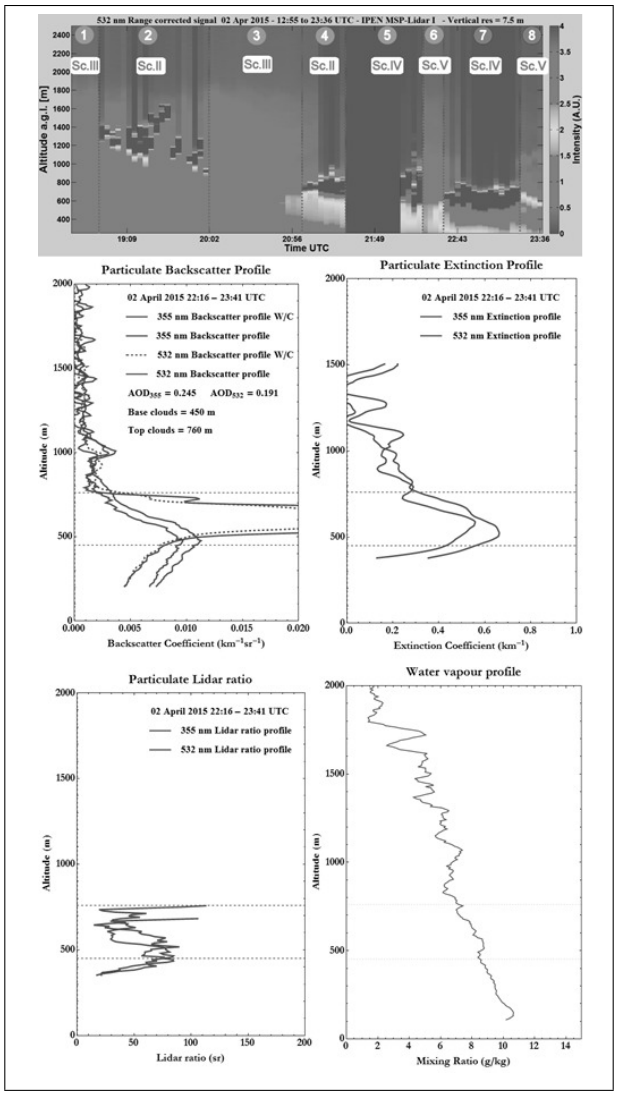

Figure 6. Periods ⑦,⑧ - Scenarios IV,V identification applied to a "curtain plot" (RCS plot) to apply the data extraction in order to observe ACI's. Below $\beta^{aer}_{355,532}$ with/out clouds.

ACKNOWLEDGMENTS

The authors would like to thank for the support given by the following funding agencies: FAPESP, CNPq. This work was also supported by the University of Granada through the contract Plan Propio. Programa 9. Convocatoria 2013 and Santander bank grant JPI2015.

Downloaded From: http://proceedings.spiedigitallibrary.org/ on 10/27/2015 Terms of Use: http://spiedigitallibrary.org/ss/TermsOfUse.aspx

REFERENCES

[1] Stocker, T., Qin, D., Plattner, G., Tignor, M., Allen, S., Boschung, J., Nauels, A., Xia, Y., Bex, V., and Midgley, P., "IPCC, Climate Change 2013: The Physical Science Basis. Fourth Assessment Report," (2013).

[2] Twomey, S., [*Introduction to the Mathematics of Inversion in Remote Sensing and Direct Measurements*], Elsevier - New York (1977).

[3] Albrecht, B., "Aerosols, Cloud Microphysics, and Fractional Cloudiness," *Science* **245**, 1227–1230 (SEP 15 1989).

[4] Penner, J., Zhang, S., and Chuang, C., "Soot and smoke aerosol may not warm climate," *JOURNAL OF GEOPHYSICAL RESEARCH-ATMOSPHERES* **108** (NOV 1 2003).

[5] Koren, I., Kaufman, Y., Remer, L., and Martins, J., "Measurement of the effect of Amazon smoke on inhibition of cloud formation," *SCIENCE* **303**, 1342–1345 (FEB 27 2004).

[6] Rosenfeld, D., "Suppression of rain and snow by urban and industrial air pollution," *SCIENCE* **287**, 1793–1796 (MAR 10 2000).

[7] Ramanathan, V., Crutzen, P., Kiehl, J., and Rosenfeld, D., "Atmosphere - Aerosols, climate, and the hydrological cycle," *SCIENCE* **294**, 2119–2124 (DEC 7 2001).

[8] Twohy, C. H., Coakley, Jr., J. A., and Tahnk, W. R., "Effect of changes in relative humidity on aerosol scattering near clouds," *JOURNAL OF GEOPHYSICAL RESEARCH-ATMOSPHERES* **114** (MAR 6 2009).

[9] Breon, F., Tanre, D., and Generoso, S., "Aerosol effect on cloud droplet size monitored from satellite," *SCIENCE* **295**, 834–838 (FEB 1 2002).

[10] Su, W., Schuster, G. L., Loeb, N. G., Rogers, R. R., Ferrare, R. A., Hostetler, C. A., Hair, J. W., and Obland, M. D., "Aerosol and cloud interaction observed from high spectral resolution lidar data," *JOURNAL OF GEOPHYSICAL RESEARCH-ATMOSPHERES* **113** (DEC 17 2008).

[11] Ansmann, A., Tesche, M., Althausen, D., Mueller, D., Seifert, P., Freudenthaler, V., Heese, B., Wiegner, M., Pisani, G., Knippertz, P., and Dubovik, O., "Influence of Saharan dust on cloud glaciation in southern Morocco during the Saharan Mineral Dust Experiment," *JOURNAL OF GEOPHYSICAL RESEARCH-ATMOSPHERES* **113** (FEB 27 2008).

[12] Guerrero-Rascado, J. and Preissler, J., "Cloud- aerosol interaction estimated by raman lidar," in [*Quinta Reunion Española de Ciencia y Tecnologia de Aerosoles*], D4–1,D4–6 (2011).

[13] Tackett, J. L. and Di Girolamo, L., "Enhanced aerosol backscatter adjacent to tropical trade wind clouds revealed by satellite-based lidar," *Geophysical Research Letters* **36**(14), n/a–n/a (2009).

[14] Eck, T. F., Holben, B. N., Reid, J. S., Arola, A., Ferrare, R. A., Hostetler, C. A., Crumeyrolle, S. N., Berkoff, T. A., Welton, E. J., Lolli, S., Lyapustin, A., Wang, Y., Schafer, J. S., Giles, D. M., Anderson, B. E., Thornhill, K. L., Minnis, P., Pickering, K. E., Loughner, C. P., Smirnov, A., and Sinyuk, A., "Observations of rapid aerosol optical depth enhancements in the vicinity of polluted cumulus clouds," *ATMOSPHERIC CHEMISTRY AND PHYSICS* **14**(21), 11633–11656 (2014).

[15] Veselovskii, I., Kolgotin, A., Griaznov, V., Müller, D., Wandinger, U., and Whiteman, D., "Inversion with regularization for the retrieval of tropospheric aerosol parameters from multi-wavelength lidar sounding," *Applied Optics* **41**, 3685–3699 (2002).

[16] Whiteman, D. N. and Melfi, S., "Cloud liquid water, mean droplet radius and number density measurements using a raman lidar," *Journal of Geophysical Research* **104**, 31411–31419 (1999).

[17] Landulfo, E., Papayannis, A., Artaxo, P., Castanho, A. D. A., de Freitas, A. Z., Souza, R. F., Junior, N. D. V., Jorge, M., Sánchez-Ccoyllo, O. R., and Moreira, D. S., "Synergetic measurements of aerosols over São Paulo, Brazil using Lidar, Sunphotometer and satelite data during dry season," ***Atmos Chem Phys* 3**, 1523–1539 (2003).

[18] Landulfo, E., Papayannis, A., Freitas, A. Z., Vieira Junior, N. D., Souza, R. F., Gonçalves, A., Castanho, A. D. A., Artaxo, P., , Sánchez-CCoyllo, O. R., Moreira, D. S., and Jorge, M. P. M. P., "Tropospheric aerosol observations in sao paulo, brazil using a compact lidar system," *Int. J. Rem. Sens.* **13**, 2797–2816 (2005).

Downloaded From: http://proceedings.spiedigitallibrary.org/ on 10/27/2015 Terms of Use: http://spiedigitallibrary.org/ss/TermsOfUse.aspx

[19] Guerrero-Rascado, J. L., Landulfo, E., Antuña, J. C., Barbosa, H. M. J., Barja, B., Bastidas, A. E., Bedoya, A. E., da Costa, R., Estevan, R., Forno, R. N., Gouveia, D. A., Jiménez, C., Larroza, E. G., Lopes, F. J. S., Montilla-Rosero, E., Moreira, G. A., Nakaema, W. M., Nisperuza, D., Otero, L., Pallotta, J. V., Papandrea, S., Pawelko, E., Quel, E. J., Ristori, P., Rodrigues, P. F., Salvador, J., Sánchez, M. F., and Silva, A., "Towards an instrumental harmonization in the framework of lalinet: dataset of technical specifications," (2014).

[20] Winker, D. M., Vaughan, M. A., Omar, A., Hu, Y., Powell, K. A., Liu, Z., Hunt, W. H., and Young, S. A., "Overview of the CALIPSO mission and CALIOP data processing algorithms," ***J. Atmos. Oceanic Technol.*** **26**, 2310–2323 (2009).

[21] Hunt, W. H., Winker, D. M., Vaughan, M. A., Powell, K. A., Lucker, P. L., and Weimer, C., "CALIPSO Lidar Description and Performance Assessment," ***J. Atmos. Oceanic Technol.*** **26**, 1214–1228 (2009).

[22] Hostetler, C. A., Liu, Z., Reagan, J., Vaughan, M. A., Winker, D. M., Osborn, M., Hunt, W. H., Powell, K. A., and Trepte, C., "**CALIOP Algorithm Theoretical Basis Document - Calibration and Level 1 data products**," *Cloud-Aerosol Lidar Infrared Pathfinder Satellite Observations* **PC-SCI-201**, 1–66 (2006).

[23] Omar, A. H., Winker, D. M., Kittaka, C., Vaughan, M. A., Liu, Z., Hu, Y., Trepte, C. R., Rogers, R. R., Ferrare, R. A., Lee, K., Kuehn, R. E., and Hostetler, C. A., "The CALIPSO automated aerosol classification and Lidar Ratio Selection Algorithm," ***J. Atmos. Oceanic Technol.*** **26**, 1994–2014 (2009).

[24] Mamouri, R. E., Amiridis, V., Papayannis, A., Giannakaki, E., Tsaknakis, G., and Balis, D. S., "Validation of CALIPSO space-borne-derived attenuated backscatter coefficient profiles using a ground-based lidar in Athens, Greece," ***Atmos. Meas. Tech.*** **2**, 513–522 (2009).

[25] Rogers, R. R., Hostetler, C. A., Hair, J., Ferrare, R. A., Liu, Z., Obland, M. D., Harper, D. B., Cook, A. L., Powell, K. A., Vaughan, M. A., and Winker, D. M., "Assessment of the CALIPSO Lidar 532 nm attenuated backscatter calibration using the NASA LaRC airborne High Spectral Resolution Lidar," ***Atmos. Chem. Phys.*** **11**, 1295–1311 (2011).

[26] Burton, S. P., Ferrare, R. A., Vaughan, M. A., Omar, A. H., Rogers, R. R., Hostetler, C. A., and Hair, J. W., "Aerosol classification from airborne HSRL and comparisons with the CALIPSO vertical feature mask," ***Atmos. Meas. Tech.*** **6**, 1397–1412 (2013).

[27] Rogers, R. R., Vaughan, M. A., Hostetler, C. A., Burton, S. P., Ferrare, R. A., Young, S. A., Hair, J. W., Obland, M. D., Harper, D. B., Cook, A. L., and Winker, D. M., "Looking through the haze: evaluating the CALIPSO level 2 aerosol optical depth using airborne high spectral resolution lidar data," ***Atmos. Meas. Tech. Discuss.*** **7**, 6141–6204 (2014).

[28] Lopes, F. J. S., Landulfo, E., and Vaughan, M. A., "Evaluating CALIPSO's 532 nm lidar ratio selection algorithm using AERONET sun photometers in Brazil," ***Atmos. Meas. Tech.*** **6**, 3281–3299 (2013).

[29] Levy, R. C., Remer, L. A., Martins, J. V., Kaufman, Y. J., Plana-Fattori, A., Redemann, J., and Wenny, B., "Evaluation of the modis aerosol retrievals over ocean and land during CLAMS.," ***J. Atmos. Sci.*** **62** (2005).

[30] Remer, L. A., Tanré, Y. J. K. D., Mattoo, S., Chu, D. A., Martins, J. V., Li, R. R., Ichoku, C., Levy, R. C., Kleidman, R. G., Eck, T. F., Vermote, E., and Holben, B. N., "The MODIS aerosol algorithm, products, and validation," ***J. Atmos. Sci.*** **62**(4), 947–973 (2005).

[31] Holben, B. N., Eck, T. F., Slutsker, I., Tanré, D., Buis, J. P., Setzer, A., Vermote, E., Reagan, J. A., Kaufman, Y. J., Nakajima, T., Lavenu, F., Jankowiak, I., and Smirnov, A., "Aeronet - A Federal Instrument Network and Data Archive for Aerosol Characterization," ***Remote Sens. Environ.*** **66**, 1–16 (1998).

[32] Dubovik, O. and King, M. D., "A flexible inversion algorithm for retrieval of aerosol optical properties from sun and sky radiance measurements," ***J. Geophys. Res.*** **105**(D16), 20673–20696 (2000).

[33] Klett, J. D., "Extinction boundary value algorithms for lidar inversion," ***Appl. Optics*** **25**, 2462 (1986).

[34] Fernald, F. G., "Analysis of atmospheric Lidar observations: some comments," ***Appl. Optics*** **23**, 652–653 (1984).

Downloaded From: http://proceedings.spiedigitallibrary.org/ on 10/27/2015 Terms of Use: http://spiedigitallibrary.org/ss/TermsOfUse.aspx